DØ note 5031-CONF

Measurement of the $t\bar{t}$ Production Cross Section at $\sqrt{s} = 1.96$ TeV in the Combined Lepton+Track and $e\mu$ Channel using 370 pb^{-1} of DØ Data

The DØ Collaboration
URL http://www-d0.fnal.gov
(Dated: March 7, 2006)

A measurement of the $t\bar{t}$ production cross section at $\sqrt{s} = 1.96$ TeV in the dilepton final state using a lepton+track selection and secondary vertex b-tagging is presented. To improve the selection efficiency, one of the two leptons from the decay of the $t\bar{t}$ pair is allowed to be identified only as an isolated track. The result is combined with a measurement in the $e\mu$ channel using the same data sample. The measurements are based on 370 pb^{-1} of data collected with the DØ experiment at the Tevatron Collider. The preliminary cross section obtained in the combined lepton+track and $e\mu$ channel is:

$$\sigma_{t\bar{t}} = 8.6^{+1.9}_{-1.7}\ (\text{stat}) \pm 1.1\ (\text{syst}) \pm 0.6\ (\text{lumi})\ \text{pb}.$$

Preliminary Results for Winter 2006 Conferences

I. INTRODUCTION

The top quark is the heaviest of the known fundamental fermions. Measurements of its production rate and properties allow for precision tests of the theory of the strong interaction, quantum chromodynamics (QCD), and may allow to detect new physics. This paper describes a measurement by the DØ collaboration of the $t\bar{t}$ pair production cross section in high energy $p\bar{p}$ collisions at $\sqrt{s} = 1.96$ TeV at the Tevatron collider.

At the Tevatron, the dominant production mode for top quarks is $t\bar{t}$ pair production, which occurs via $q\bar{q}$ annihilation (85%) or gluon fusion (15%). Calculations of the $t\bar{t}$ cross section at $\sqrt{s} = 2$ TeV using QCD next-to-leading order (NLO) range from 6.7 to 7.5 pb [1–3], if a top mass of 175 GeV is used. At next-to-next-to-leading order (NNLO), the predicted cross section at $\sqrt{s} = 1.96$ TeV is 6.77 ± 0.42 pb [3].

In the standard model, the top quark decays with almost 100% probability to a W boson and a b-quark. The $t\bar{t}$ final state is completely determined by the decays of the two W bosons. Experimentally, the most relevant channels are the "dilepton" channels where each of the W bosons decay leptonically into an electron or a muon (ee, $\mu\mu$, $e\mu$) and a corresponding neutrino, and the "lepton+jets" channels where one of the W bosons decays hadronically into two jets (e+jets, μ+jets).[1] In all channels, two additional jets arise from the fragmentation of the b-quarks.

In order to measure the $t\bar{t}$ production cross section, dedicated selections designed to enhance the signal content have to be applied. The measurement presented in this paper uses a "lepton+track" selection, where one of the leptons is identified as an isolated track in order to improve the statistical sensitivity. The candidate events are required to have one well identified high p_T lepton (electron or muon), one high p_T isolated track and large $\not\!\!E_{\rm T}$.

The purity of the signal sample can be enhanced by exploiting differences in the heavy flavor content of top quark events as compared to background events. This paper describes an analysis which uses a secondary vertex b-tagging algorithm to identify the b-jets from the top quark decays.

The data sample used for this measurement consists of data collected with the DØ detector, corresponding to an integrated luminosity of approximately 370 pb^{-1}. The measurement in the lepton+track channel is combined with a measurement in the $e\mu$ channel [4] using the same data sample.

II. THE DØ DETECTOR

The DØ Run II detector [5, 6] is comprised of the following main components: the central tracking system, the liquid-argon/uranium calorimeter, and the muon spectrometer.

The central tracking system includes a silicon microstrip tracker (SMT) and a central fiber tracker (CFT), both located inside a 2 T superconducting solenoid magnet. The SMT is designed to provide efficient tracking and vertexing capability at pseudorapidities of $|\eta| < 3$. The system has a six-barrel longitudinal structure, each with a set of four layers arranged axially around the beampipe, and interspersed with 16 radial disks. A typical pitch of 50-80 μm of the SMT strips allows a precision determination of the three-dimensional track impact parameter with respect to the primary vertex which is the key component of the lifetime based b-jet tagging algorithms. The CFT has eight coaxial barrels, each supporting two doublets of overlapping scintillating fibers of 0.835 mm diameter, one doublet being parallel to the collision axis, and the other alternating by $\pm 3^o$ relative to the axis.

The calorimeter is divided into a central section (CC) providing coverage out to $|\eta| \approx 1$, and two end calorimeters (EC) extending coverage to $|\eta| \approx 4$ all housed in separate cryostats. Scintillators placed between the CC and EC provide sampling of showers at $1.1 < |\eta| < 1.4$.

The muon system, covering $|\eta| < 2$, resides beyond the calorimetry, and consists of three layers of tracking detectors and scintillating trigger counters. Moving radially outwards, the first layer is placed inside the 1.8 T toroid magnets, and the two following layers are located outside the magnets.

III. MONTE CARLO MODELS FOR SIGNAL AND BACKGROUND SAMPLES

The $t\bar{t}$ signal expectations are determined from a full Monte Carlo simulation of top-antitop events. This simulation utilizes events generated at $\sqrt{s} = 1.96$ TeV with the ALPGEN 1.2 [7] matrix element generator assuming a top mass of 175 GeV and the parton distribution function set CTEQ 6.1M [8]. These events are processed through PYTHIA 6.2 [9] to provide higher order QCD evolution (i.e. gluon radiation and fragmentation) and short lived particle decays.

[1] Unless otherwise explicitly stated a reference to a particle species can also be taken to refer to the anti-particle.

EvtGen [10] is used to model the decays of b hadrons. The W bosons are both decayed to a lepton-neutrino pair, including all τ final states. The generated events are processed through a GEANT [11] simulation of the DØ detector providing tracking hits, calorimeter cell energy and muon hit information. Multiple interactions are added to all events according to a Poisson distribution with a mean which is determined from the average instantaneous luminosity. The same reconstruction is applied to data and Monte Carlo events.

The main backgrounds are evaluated using a combination of data and Monte Carlo. The main background in the lepton+track channel, ($Z/\gamma* \to ee/\mu\mu$) with fake $\not\!\!E_{\rm T}$, as well as the largest physics background, ($Z/\gamma* \to \tau\tau$), are generated using ALPGEN interfaced to PYTHIA. The other physics background considered, WW, is studied using a $WW \to \ell\ell$ sample produced with PYTHIA. In all above cases, τ leptons can decay both leptonically and hadronically.

Additional smearing of the momenta of muons, electrons, tracks and jets is applied according to the observed resolution in data. Remaining discrepancies in the description of the object reconstruction and identification between the simulation and the data were taken into account with correction factors derived by comparing the efficiencies measured in $Z \to \ell\ell$ data events to the ones obtained from the simulation. Trigger efficiencies derived on data were also applied to the simulated events.

IV. OBJECT IDENTIFICATION

Electrons are identified as clusters in the electromagnetic layers of the calorimeter found within $\Delta R = \sqrt{(\Delta\phi)^2 + (\Delta\eta)^2} = 0.4$ using a cone algorithm. These clusters are further required to be isolated from nearby hadronic energy, to satisfy a loose shower shape selection, and to satisfy a loose match to a central track. In the final selection a multiparameter likelihood discriminant (e_{lh}) is used which compares the probabilities for a certain candidate to be either a real electron or background (i.e. a highly electromagnetic jet). Electrons measured in the central ($|\eta| < 1.1$) and the forward ($1.5 < |\eta| < 2.5$) regions are used in this measurement. Electromagnetic energy scale corrections are derived using electrons reconstructed from Z boson decays.

Muons are built from a track segment in the inner muon layer matching a segment formed from hits in the outer two layers. The track formed in the muon system also has to be matched to a central track, and the overall χ^2 per degree of freedom of the track fit is required to be less than 4. Timing cuts to reject cosmic ray muons are applied based on muon scintillator signals. Muons originating from decays of W or Z bosons are identified by requiring that the muon is isolated from other activity in the calorimeter and the tracking detectors.

Tracks are reconstructed from information in the silicon tracker and the central fiber tracker. Only tracks with $\eta < 2$ are used. The χ^2 per degree of freedom of the track fit is required to be less than 4. The candidate track is selected by requiring that the track is isolated from other activity in the tracking detectors. The track is considered isolated if the total transverse momentum of all other tracks in a cone with radius $\Delta R = 0.5$ around the candidate track is less than 10% of the candidate track p_T. In addition, the candidate track is required to be separated from any reconstructed jet.

Candidate electrons, muons and tracks are required to originate from the primary vertex. This is ensured by a small impact parameter significance in the transverse plane and a small distance to the primary vertex in the z-direction.

Jets are reconstructed using an iterative algorithm, which integrates the energy observed in the calorimeter in a cone with radius $\Delta R = 0.5$. These jets are required to be in the region $|\eta| < 2.5$. The energy of the jets after reconstruction is corrected to represent the true jet energy. An equivalent correction is derived for Monte Carlo events.

The total missing transverse energy $\not\!\!E_{\rm T}$ is used to detect the presence of neutrinos with substantial p_T in the event. In the events where the $\not\!\!E_{\rm T}$ is aligned with the candidate track the transverse momentum of the candidate track is added to the $\not\!\!E_{\rm T}$ calculation if the track does not point to any reconstructed lepton.

The reconstruction of the primary vertex, which is crucial for b-tagging, is made from tracks which satisfy a set of basic quality criteria. Events are rejected if the primary vertex is not found within the fiducial region of the silicon tracker, or if less than 3 tracks are used in its determination.

The DØ trigger is a three-level trigger system. Level 1 is a hardware trigger, while levels 2 and 3 are software filters. Events in the e + track channel are required to pass a single electron or electron+jets trigger. In the μ + track channel, the events are required to pass a single muon or muon+jets trigger.

V. PRESELECTION OF $t\bar{t}$ EVENTS

The final state in the lepton+track channel is characterized by a high p_T isolated lepton (electron or muon), a high p_T isolated track, large missing transverse energy and two b-jets. The following transverse momentum cuts are used: electron, muon and track $p_T > 15$ GeV and jet $p_T > 20$ GeV. The $\not\!\!E_{\rm T}$ selection is different in the e + track and μ + track channels. The $\not\!\!E_{\rm T}$ cut is also different depending on whether the invariant mass of the lepton and the

track $M_{\ell,trk}$ is inside or outside the Z boson mass window. In the $e+$track channel the signal events are required to have $\not\!\!E_{\rm T} > 20$ GeV for $70 \leq M_{e,trk} \leq 100$ GeV and $\not\!\!E_{\rm T} > 15$ GeV for $M_{e,trk} > 100$ GeV or $M_{e,trk} < 70$ GeV. In the $\mu+$track channel the events are required to have $\not\!\!E_{\rm T} > 35$ GeV for $70 \leq M_{\mu,trk} \leq 110$ GeV and $\not\!\!E_{\rm T} > 25$ GeV for $M_{\mu,trk} > 110$ GeV or $M_{\mu,trk} < 70$ GeV. Only events with one or more jets are considered.

Events with a reconstructed high p_T isolated electron and a high p_T isolated muon in the final state ($e\mu$ events) do not suffer from the $Z \to \ell\ell$ background. Using b-tagging to suppress background events is unnecessary for these events. The $e\mu$ events are therefore explicitly vetoed in the lepton+track analysis. This allows for a straightforward combination of the lepton+track cross section measurement and a measurement in the $e\mu$ channel using topological selections.

Figures 1 and 2 show the agreement between the observed and predicted $\not\!\!E_{\rm T}$ and leading lepton p_T in the lepton+track signal sample before the b-tagging requirement has been applied.

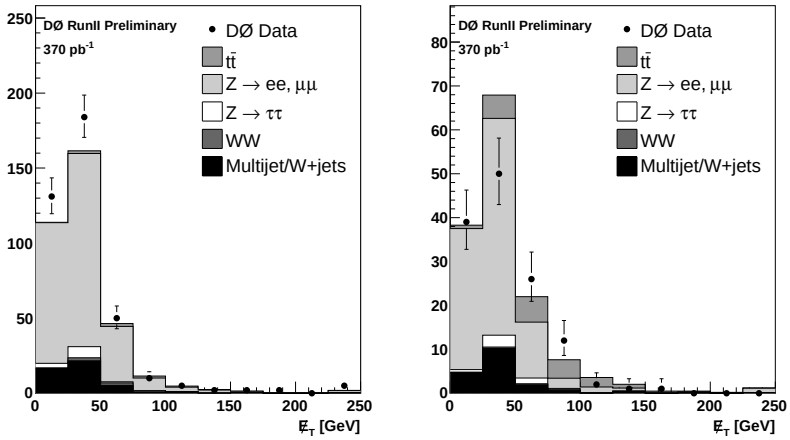

FIG. 1: Observed and predicted $\not\!\!E_{\rm T}$ before b-tagging in the lepton+track channel 1-jet bin (left) and the lepton+track channel 2-jet bin (right).

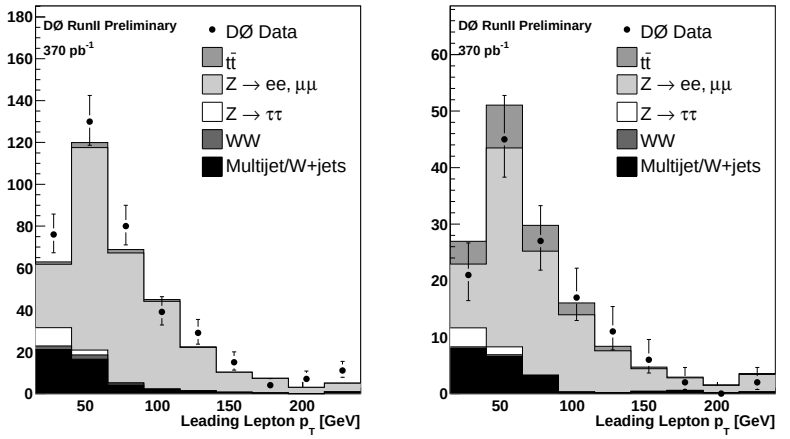

FIG. 2: Observed and predicted leading lepton p_T before b-tagging in the lepton+track channel 1-jet bin (left) and the lepton+track channel 2-jet bin (right).

VI. THE SECONDARY VERTEX TAGGING ALGORITHM

The $t\bar{t}$ final state contains two b-jets, while jets in background events originate predominantly from light quarks or gluons. Requiring at least one jet in the event to be b-tagged is therefore a very powerful discriminant between signal and background. The b-tagging algorithm used in this measurement is the secondary vertex tagging algorithm (SVT), which explicitly reconstructs vertices that are displaced from the primary vertex. In the fitting procedure, the SVT uses only good quality tracks that have an impact parameter significance > 3. Only secondary vertices which are displaced from the primary vertex in the plane transverse to the beam line by more than 7 standard deviations are considered in this measurement.

The performance of the algorithm has been extensively studied in data. The b-tagging efficiency for semileptonically decaying b quarks (semileptonic b-tagging efficiency) is measured in a data sample enhanced in heavy flavor jets by requiring at least one jet in each event to contain a muon. The b-tagging efficiency for inclusively decaying b quarks (inclusive b-tagging efficiency) is obtained by applying correction factors derived from Monte Carlo. The c-tagging efficiency cannot be directly measured in data. It is obtained from the semileptonic b-tagging efficiency in data, corrected by the ratio of inclusive c-tagging efficiency to semileptonic b-tagging efficiency in Monte Carlo. The probability to tag a light-flavor jet, the so called "mistag rate", is measured in data. Events where the secondary vertex has a negative decay length, meaning that the tracks forming the secondary vertex meet behind the primary vertex with respect to the jet axis, are used to determine the mistag rate. The b- and c-tagging efficiency and the mistag rate are parameterized as functions of jet p_T and η. These parameterizations are applied to the Monte Carlo events to predict the probability for $t\bar{t}$ events to be b-tagged.

A. Physics Backgrounds

The selection efficiencies for the physics backgrounds $Z/\gamma^* \to \tau\tau$ and WW are estimated using Monte Carlo samples generated by ALPGEN interfaced to PYTHIA. The number of $Z/\gamma^* \to \tau\tau$ events before selections is normalized using the $Z \to ee, \mu\mu$ cross section observed in data. For the WW process, the NLO cross section is used [12].

The b-tagging efficiency for $Z/\gamma^* \to \tau\tau$ is taken to be the same as for $Z/\gamma^* \to ee, \mu\mu$ events. The b-tagging efficiency for WW events is assumed to be the same as for W+jets event.

B. Missing E_T Instrumental Background

Detector resolution effects can give rise to fake $\not\!\!E_{\rm T}$. In the lepton+track channel, the primary instrumental background arises from fake $\not\!\!E_{\rm T}$ in $Z/\gamma^* \to ee, \mu\mu$ events.

Once electron, muon and jet resolutions in the Monte Carlo simulation have been adjusted to the measured resolutions in data, the $\not\!\!E_{\rm T}$ spectrum for $Z \to \ell\ell$ events in Monte Carlo agrees well with that observed in data. The $Z \to \ell\ell$ background is normalized using the ratio of the observed to predicted number of events in the low $\not\!\!E_{\rm T}$ region.

The tagging probability is determined from $Z \to \ell\ell$ events with low $\not\!\!E_{\rm T}$ in data. A systematic uncertainty is introduced for the assumption that $Z \to \ell\ell$ events with low and high $\not\!\!E_{\rm T}$ have the same tagging probability.

C. Lepton and Track Instrumental Backgrounds

Additional backgrounds arise from multijet and W+jets events. In most of these events the isolated lepton, the isolated track or both are the result of misreconstruction.

Fake electrons can arise from misreconstructed jets with large electromagnetic fraction. Fake isolated muons can arise from muons produced in a jet when the surrounding jet is not reconstructed. Isolated high p_T tracks can be faked by jets which are not properly reconstructed.

The instrumental lepton and track backgrounds before b-tagging are all estimated using a four-step matrix method. It makes use of four samples with different fractions of signal and background. In the *tight lepton-tight track* sample, all selection criteria except the b-tagging requirement have been applied. In the three remaining samples (denoted *loose lepton-tight track*, *tight lepton-loose track* and *loose lepton-loose track*) either the cuts on the lepton and/or track have been loosened. If the efficiencies of the tight lepton/track cuts relative to the loose cuts are known for true as well as fake isolated leptons and tracks, one can write down a system of four equations and solve for the number of events with true and fake isolated leptons and tracks. The tagging probability for W+jets (multijet) events is estimated in a sample with an isolated lepton and high (low) $\not\!\!E_{\rm T}$.

VII. THE SIGNAL ACCEPTANCE

The preselection efficiency for $t\bar{t}$ events is estimated using the Monte Carlo sample described in Sec. III. The tagging probability is estimated by taking the jet kinematics from the $t\bar{t}$ Monte Carlo sample and folding in the per jet tagging efficiency parameterizations determined on data (see Sec. VI).

VIII. SAMPLE COMPOSITION AFTER b-TAGGING

Shown in Tab. 1 is the summary of the number of expected and observed events after b-tagging. The expected number of $t\bar{t}$ events is derived assuming a $t\bar{t}$ cross section of 7 pb. The summary of the observed and predicted number of b-tagged events is also shown in Fig. 3. Kinematic distributions are shown in Figs. 4-6 for the lepton+track channel and the combined lepton+track and $e\mu$ channel.

	e + track		μ + track	
	Njets = 1	Njets $\geq$ 2	Njets = 1	Njets $\geq$ 2
	Expected number of tagged events			
WW	0.037 ± 0.002	0.010 ± 0.002	0.016 ± 0.001	0.009 ± 0.002
$Z/\gamma^* \to \tau\tau$	0.09 ± 0.02	0.13 ± 0.02	0.03 ± 0.01	0.09 ± 0.02
$Z/\gamma^* \to ee, \mu\mu$	1.49 ± 0.04	2.35 ± 0.06	1.44 ± 0.04	1.86 ± 0.06
Multijet/W+jets	0.36 ± 0.06	0.35 ± 0.07	0.08 ± 0.02	0.05 ± 0.03
Total background	1.97 ± 0.08	2.83 ± 0.09	1.57 ± 0.05	2.00 ± 0.07
Tot. uncertainty (stat+syst) on bkg	+0.91 −0.85	+0.87 −0.64	+0.77 −0.77	+0.51 −0.49
$t\bar{t}$	1.55 ± 0.03	6.59 ± 0.07	0.92 ± 0.02	4.74 ± 0.06
Total	3.53 ± 0.08	9.4 ± 0.1	2.49 ± 0.05	6.74 ± 0.09
Tot. uncertainty (stat+syst) on $t\bar{t}$ + bkg	+0.99 −0.86	+0.99 −0.85	+0.83 −0.77	+0.67 −0.64
	Observed number of tagged events			
Data	7	9	1	6

TABLE 1: Number of observed and predicted events in the both channels after tagging. Unless explicitly stated the uncertainties quoted are statistical only.

IX. LEPTON+TRACK AND $e\mu$ CHANNEL COMBINATION

The combined cross section was estimated by minimizing the sum of the negative log-likelihood functions for each of the five individual channels: $e\mu$, e+track (μ+track) with one jet and e+track (μ+track) with two or more jets. The functional form of the likelihood function for $e\mu$ channel is described in [4]. There is no overlap between the lepton+track and $e\mu$ samples since the lepton+track analysis includes an $e\mu$ veto. The cross sections in the lepton+track and $e\mu$ channels, and the combined cross section for $m_t = 175$ GeV are

$$\begin{aligned}
\text{lepton+track}: \ \sigma_{t\bar{t}} &= 7.1\ ^{+2.6}_{-2.2}\ (\text{stat})\ ^{+1.3}_{-1.3}\ (\text{syst})\ \pm 0.4\ (\text{lumi})\ \text{pb}. \\
e\mu: \ \sigma_{t\bar{t}} &= 10.2\ ^{+3.1}_{-2.6}\ (\text{stat})\ ^{+1.6}_{-1.3}\ (\text{syst})\ \pm 0.7\ (\text{lumi})\ \text{pb}. \\
\text{comb}: \ \sigma_{t\bar{t}} &= 8.6^{+1.9}_{-1.7}\ (\text{stat})\ ^{+1.1}_{-1.1}\ (\text{syst})\ \pm 0.6\ (\text{lumi})\ \text{pb}.
\end{aligned}$$

In the top quark mass range of 170-180 GeV, the measured cross section changes by 0.085 pb per GeV.

The systematic uncertainty on the cross section measurement is obtained by varying the backgrounds and efficiencies, within their errors, with all correlations between the channels and between the different classes of backgrounds taken into account. Table 2 summarizes the contributions from the different sources of systematic uncertainties to the total systematic uncertainty on the cross sections.

X. SUMMARY

Using the combined lepton+track and $e\mu$ channel, the cross section for $t\bar{t}$ pair production in $p\bar{p}$ collisions at $\sqrt{s} = 1.96$ TeV is measured to be: $\sigma_{t\bar{t}} = 8.6^{+1.9}_{-1.7}\,(\text{stat})\,^{+1.1}_{-1.1}\,(\text{syst}) \pm 0.6\,(\text{lumi})$ pb. The data is in good agreement with the prediction from the standard model using perturbative QCD calculations.

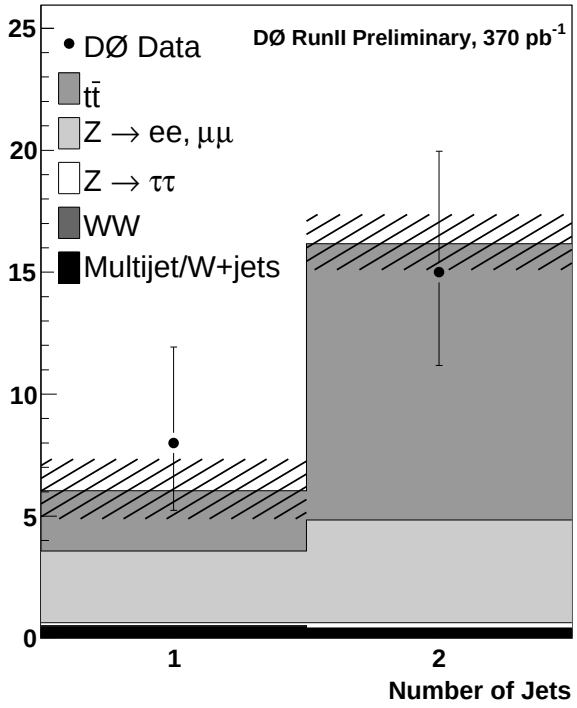

FIG. 3: The number of observed and predicted b-tagged events in the lepton+track channel as a function of the number of jets. The hashed area represents the total uncertainty on the prediction.

Acknowledgments

We thank the staffs at Fermilab and collaborating institutions, and acknowledge support from the DOE and NSF (USA); CEA and CNRS/IN2P3 (France); FASI, Rosatom and RFBR (Russia); CAPES, CNPq, FAPERJ, FAPESP and FUNDUNESP (Brazil); DAE and DST (India); Colciencias (Colombia); CONACyT (Mexico); KRF and KOSEF (Korea); CONICET and UBACyT (Argentina); FOM (The Netherlands); PPARC (United Kingdom); MSMT (Czech Republic); CRC Program, CFI, NSERC and WestGrid Project (Canada); BMBF and DFG (Germany); SFI (Ireland); Research Corporation, Alexander von Humboldt Foundation, and the Marie Curie Program.

[1] E. Berger and H. Contopanagos, Phys. Rev. D **57**, 253 (1998).
[2] R. Bonciani, S. Catani, M. Mangano and P. Nason, Nucl. Phys. B529, 424 (1998).
[3] N. Kidonakis and R. Vogt, Phys. Rev. D **68**, 114014 (2003).
[4] DØ Collaboration, *Measurement of the $t\bar{t}$ Production Cross Section at $\sqrt{s}$ = 1.96 TeV in Dilepton Final States using 370 pb^{-1} of DØ Data*, DØ Note 4850-CONF, July 2005.
[5] T. LeCompte and H.T. Diehl, "The CDF and DØ Upgrades for RunII", Ann. Rev. Nucl. Part. Sci. **50**, 71 (2000).
[6] DØ Collaboration, hep-physics/0507191.
[7] M.L. Mangano et al., JHEP 0307:001, 2003, hep-ph/0206293.
[8] J. Pumplin, D. R. Stump, J. Huston, H. L. Lai, P. Nadolsky, W. K. Tung, hep-ph/0201195.
[9] T. Sjöstrand et al., LU TP 01-21, hep-ph/0108264.
[10] http://charm.physics.ucsb.edu/people/lange/EvtGen/
[11] R. Brun and F. Carminati, CERN Program Library Long Writeup W5013 1993.
[12] J.M. Campbell and R.K. Ellis, Phys Rev D **60**, 113006 (1999).

Source	$e\mu$		l+track		l+track+$e\mu$	
Primary Vertex	-0.5	$+0.5$	-0.6	$+0.7$	-0.6	$+0.6$
Electron identification	-3.0	$+4.0$	-2.8	$+4.2$	-2.9	$+3.7$
Electron trigger	-4.9	$+5.5$	-1.3	$+1.7$	-0.7	$+3.6$
Muon identification	-5.9	$+6.3$	-3.2	$+3.4$	-4.4	$+4.5$
Muon trigger	-5.7	$+8.4$	-1.8	$+2.2$	-3.6	$+5.0$
Track identification	0	0	-3.8	$+4.2$	-1.9	$+2.0$
Jet energy scale	-5.5	$+5.2$	-13.7	$+8.9$	-8.5	$+6.6$
Jet identification	-3.5	$+4.7$	-2.5	$+0.1$	-3.2	$+2.2$
Jet resolution	-2.4	$+4.7$	-2.3	$+0.6$	-2.4	$+1.7$
Jet trigger	0	0	-0.6	$+0.7$	-0.2	$+0.3$
e_{lh} fit and opposite sign req.	-3.7	$+4.2$	0	0	-1.7	$+1.9$
$t\bar{t}$ tagging probability	0	0	-3.9	$+4.1$	-2.1	$+2.2$
Multijet/W+jets background	0	0	-1.3	$+0.8$	-0.6	$+0.3$
WW background	-2.4	$+2.4$	-0.6	$+0.6$	-1.6	$+1.6$
Z background	-0.7	$+0.7$	-9.9	$+13.0$	-4.0	$+5.2$
Other	-2.2	$+2.2$	-2.0	$+2.3$	-2.0	$+2.2$
Total	-12.4	$+16.1$	-18.9	$+18.5$	-12.8	$+13.3$

TABLE 2: Summary of the relative systematic uncertainties (in %) on the $e\mu$, lepton+track and combined result.

APPENDIX A: KINEMATIC DISTRIBUTIONS

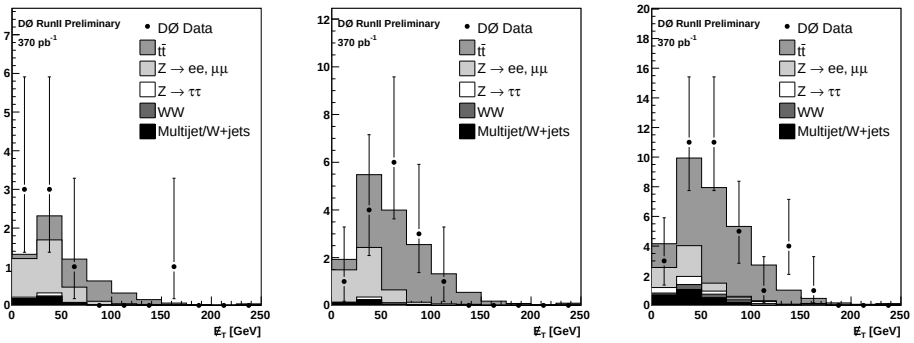

FIG. 4: Observed and predicted $\not\!\!E_{\rm T}$ in the lepton+track channel 1-jet bin (left), the lepton+track channel 2-jet bin (middle) and the combined lepton+track and $e\mu$ channel 2-jet bin (right).

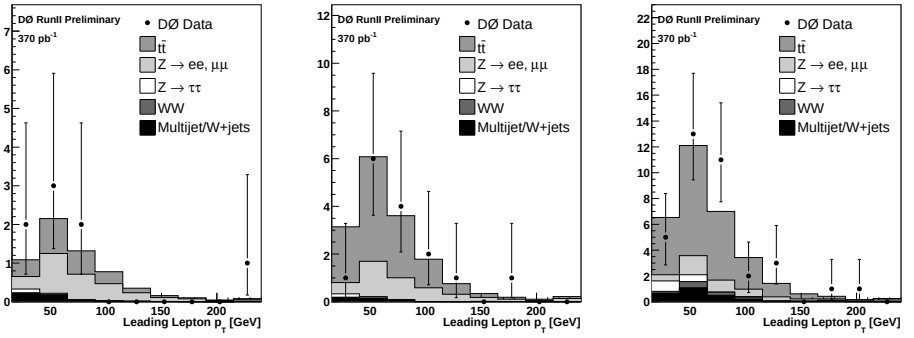

FIG. 5: Observed and predicted leading lepton p_T in the lepton+track channel 1-jet bin (left), the lepton+track channel 2-jet bin (middle) and the combined lepton+track and $e\mu$ channel 2-jet bin (right).

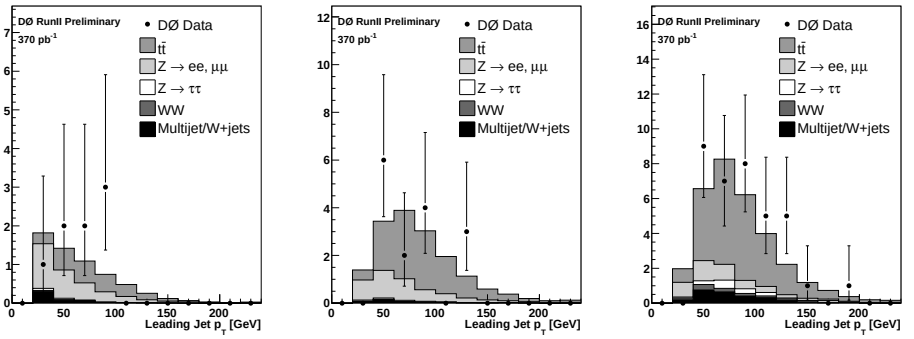

FIG. 6: Observed and predicted leading jet p_T in the lepton+track channel 1-jet bin (left), the lepton+track channel 2-jet bin (middle) and the combined lepton+track and $e\mu$ channel 2-jet bin (right).